AAS 03-040

American Astronautical Society

First Results from a Hardware-in-the-Loop Demonstration of Closed-Loop Autonomous Formation Flying

E. Gill, B. Naasz*, T. Ebinuma†

German Aerospace Center (DLR), German Space Operations Center, Münchener Str. 20, D-82230 Wessling, Germany, eberhard.gill@dlr.de, Fax +49 (8153) 28-1450, Phone +49 (8153) 28-2993

**NASA Goddard Space Flight Center, Greenbelt, Maryland 20771, U.S.A.*

†*Center for Space Research, University of Texas at Austin, Austin, Texas 78712, U.S.A.*

26th ANNUAL AAS GUIDANCE AND CONTROL CONFERENCE

February 5-9, 2003
Breckenridge, Colorado

Sponsored by
Rocky Mountain Section

American Astronautical Society
Rocky Mountain Section

AAS Publications Office, P.O. Box 28130 - San Diego, California 92198

AAS 03-040

FIRST RESULTS FROM A HARDWARE-IN-THE-LOOP DEMONSTRATION OF CLOSED-LOOP AUTONOMOUS FORMATION FLYING

Eberhard Gill, Bo Naasz, Takuji Ebinuma

A closed-loop system for the demonstration of autonomous satellite formation flying technologies using hardware-in-the-loop has been developed. Making use of a GPS signal simulator with a dual radio frequency outlet, the system includes two GPS space receivers as well as a powerful onboard navigation processor dedicated to the GPS-based guidance, navigation, and control of a satellite formation in real-time. The closed-loop system allows realistic simulations of autonomous formation flying scenarios, enabling research in the fields of tracking and orbit control strategies for a wide range of applications.

The autonomous closed-loop formation acquisition and keeping strategy is based on Lyapunov's direct control method as applied to the standard set of Keplerian elements. This approach not only assures global and asymptotic stability of the control but also maintains valuable physical insight into the applied control vectors. Furthermore, the approach can account for system uncertainties and effectively avoids a computationally expensive solution of the two point boundary problem, which renders the concept particularly attractive for implementation in onboard processors.

A guidance law has been developed which strictly separates the relative from the absolute motion, thus avoiding the numerical integration of a target trajectory in the onboard processor. Moreover, upon using precise kinematic relative GPS solutions, a dynamical modeling or filtering is avoided which provides for an efficient implementation of the process on an onboard processor. A sample formation flying scenario has been created aiming at the autonomous transition of a Low Earth Orbit satellite formation from an initial along-track separation of 800 m to a target distance of 100 m. Assuming a low-thrust actuator which may be accommodated on a small satellite, a typical control accuracy of less than 5 m has been achieved which proves the applicability of autonomous formation flying techniques to formations of satellites as close as 50 m.

INTRODUCTION

As the objectives in earth observation, communication and navigation become increasingly complex, single satellite solutions may no longer be adequate. Instead, multi-satellite systems may be required which are implemented as formations, constellations, or swarms. The orbit control of near-term satellite formations, such as the presently operated US-German GRACE mission (Ries et al. 2002) or the planned American TechSat-21 project (Chien et al. 2001) may well be operated by a conventional

ground control center. In contrast, missions planned for the next decade, like the ESA missions XEUS (Bleeker & Mendez 2002) and Darwin (Chapman & Gillett 2002), call for an onboard autonomous relative navigation control. Research and development in the field of autonomous relative navigation and control is thus an essential contribution to a forward-looking orientation in contemporary space flight technology.

The described closed-loop system for formation acquisition and keeping using hardware-in-the-loop attempts to demonstrate the feasibility of autonomous formation control in a realistic environment. This comprises the use of real GPS signals with typical systematic errors such as ionosphere errors and GPS broadcast ephemeris errors, real GPS measurements with their associated statistical errors, as well as execution of the control task on a flight processor. Moreover, the demonstration accounts for the complex dynamics of satellite orbital motion which renders the demonstration as realistic as possible. In the next chapter, the architecture and the constituents of the closed-loop system are described, followed by an introduction to Lyapunov's stability analysis method and its specific adaptation to the formation flying problem. In the last chapter, the results of an autonomous formation flying demonstration are presented which prove the feasibility of the proposed concept. Finally, benefits and drawbacks associated with the herein adopted formulation of Lyapunov's stability method are discussed.

SIMULATION SYSTEM DESCRIPTION

System Architecture

The formation flight system (Fig. 1) has been established at the Formation Flying Test Bed (Leitner 2001) of NASA's Goddard Space Flight Center. It consists of a GPS signal generator, two GPS ORION receivers, a Power PC navigation processor, a remote control PC as well as a monitoring Laptop. Communications between the system components apply both serial and parallel interfaces as well as radio frequency links.

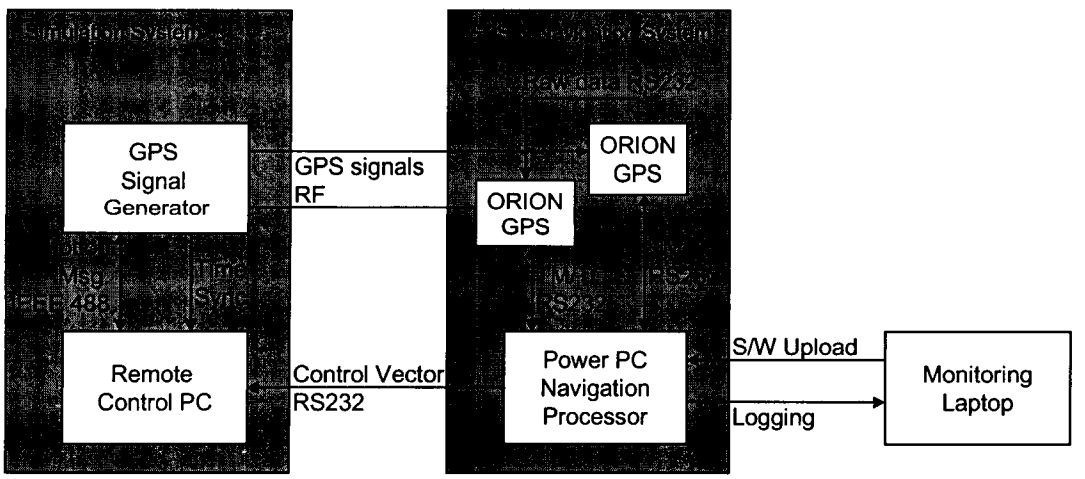

Fig. 1. Closed-loop autonomous formation control setup.

The system uses a Spirent STR4760 GPS signal simulator (GSS) capable of simulating L1 signals for 2 vehicles on up to 16 channels each. Upon running a closed-loop

formation simulation with two satellites, the GSS is provided every 100 ms with two satellite motion messages from an external Remote Control PC, which comprise the current spacecraft position, velocity, acceleration, and jerk values.

Two GPS Orion receivers, described in more detail in a separate section below, are directly connected to the simulator R/F output of the GSS via co-axial cables and low noise amplifiers. This is considered an acceptable restriction and avoids the detrimental effects of a direct signal transmission inside the laboratory environment. In the described demonstrations, absolute GPS position and velocity fixes are used as well as their mutual relative state. The latter is based on the exchange of raw measurements via a dedicated serial data link (Montenbruck et al. 2002). Thus, no raw GPS measurements have to be processed on the flight computer. Therefore this study will focus on the autonomous formation control problem, considerably reducing the complexity of the onboard processor software.

Both GPS receivers were connected to two RS-232 ports of the Power PC navigation processor, which is described below in more detail. The navigation processor acts as flight computer on one of the two satellites and executes the formation flight guidance and control functions. As output, a control request message may be issued which specifies the time and velocity increment associated with a single thruster activation. This message is in turn transmitted via the third RS-232 port of the navigation processor for application within the remote control PC. The monitoring laptop allows a direct upload of the Real-time Formation Flight (RFF) application software to the processor via a dedicated parallel port of the processor board. Monitoring of the control process at run-time and logging on the monitoring laptop is conveniently supported making use of a dedicated serial interface.

Control requests issued from the navigation processor are received by the Remote Control PC. This PC numerically integrates the satellite state vectors and adds the velocity increments of the control requests, representing the thruster activities, to the orbital velocity of the satellites. The Remote Control PC also controls the GPS signal simulator through the provision of the current satellite states in specific motion messages at a rate of 10 Hz, thus closing the loop of the autonomous formation control system. To this end, an IEEE 488 interface is applied and time synchronization is established using a dedicated timer card.

GPS Receiver Hardware

The GPS Orion receiver, developed by DLR's German Space Operations Center, is based on the Mitel (now Zarlink) GP2000 chipset. It comprises a GP2015 R/F front end and DW9255 saw filter, a GP2021 correlator as well as an ARM60B 32-bit microprocessor (Montenbruck et al. 2001). It provides C/A code tracking on 12 channels at the L1 frequency and operates with an active antenna having a total gain of roughly 28 dB. The receiver consumes a total of 2.4 W when accounting for the main receiver board as well as the interface board. The latter provides line drivers for the two I/O ports as well as a rechargeable NiCd battery to maintain the real-time clock and non-volatile memory inside the receiver while disconnected from the main power supply.

The receiver provides navigation solutions, smoothed and unsmoothed C/A code pseudoranges and integrated L1 carrier phase measurements. The carrier phase measurements are obtained using a 3rd order (frequency lock loop (FLL) assisted) phase

lock loop (PLL), which offers good signal acquisition performance as well as accurate tracking of the carrier phase under high dynamics. Upon connecting the two Orions, the receivers process single difference measurements to obtain their mutual relative state (Montenbruck et al. 2002). This differential processing scheme allows a high level of common error cancellation while minimizing the resulting noise by appropriate use of carrier phase measurements.

Flight Computer

The navigation processor features an industrial Power PC 823e processor operated at 48 MHz clock rate (without floating point support), which provides a performance of 66 MIPS. A total of 8 MB of DRAM memory are available as well as 8 MB of shadow mirror memory and 128 kB of ROM to save critical run-time parameters (Montenegro 2001). The DRAM is parity protected and duplicated which allows for error detection and correction. The application software can be directly uploaded to the processor via a parallel connection located at the processor board. Run-time monitoring and logging on a remote PC is conveniently supported making use of a dedicated RS-232 interface.

The navigation processor is running under the real-time operating system BOSS, which separates the kernel run-time system and a hardware dependant layer. BOSS is a preemptive multitasking operating system well suited for real-time and onboard applications. Processes are executed as separate threads, which are controlled by a central scheduler based on pre-assigned priorities and timers. In this way, short and high-priority activities (e.g. commanding) can be separated from computation intensive tasks with long duty cycles (e.g. orbit determination). BOSS is implemented in C++ and provides a C++ interface for the software application development (Leung et al. 2002). The Power PC board and the real-time operating system BOSS were developed for the German BIRD small satellite mission and have been successfully operating onboard BIRD since October 2001.

LYAPUNOV CONTROL THEORY

Theory Outline

Since the equations of satellite motion are non-linear, the relative motion of a satellite formation is governed by non-linear equations as well. Although linear control may in general be applied to non-linear systems and may even turn out to be highly efficient, non-linear control strategies can be beneficial in various ways. In general, they may improve the control robustness to parametric uncertainty, enable control for systems not controllable by linear approaches, and preserve and exploit physical insight.

Out of the many non-linear control theories, Lyapunov's direct method (second method) appears as a feasible approach to the problem of relative motion control. Here, the control drives the system dynamics along a direction opposite to the gradient of a specific Lyapunov function in such a way, that the current state approaches and finally reaches the terminal state conditions. Although Lyapunov's method is necessarily neither time-optimal nor fuel-optimal, it provides globally asymptotically stable solutions to linear and non-linear systems. As the computation of the feedback control requires only a moderate computational effort, it is especially suited for real-time and onboard applications. Furthermore, large matrices as in predictive control strategies (Rossi &

Lovera 2002) are avoided since the involved matrix/vector dimensions are just of the size of the state of the dynamical system.

Lyapunov's theory analyzes the stability of dynamical systems described by *n*-dimensional first-order equations of the form

$$\dot{\boldsymbol{x}} = \boldsymbol{f}(\boldsymbol{x}) \qquad \boldsymbol{x}, \dot{\boldsymbol{x}}, \boldsymbol{f} \in \boldsymbol{R}^n \tag{1}$$

where dotted symbols denote derivatives with respect to time. If we select an *m*-dimensional feedback control vector $\boldsymbol{u}(\boldsymbol{x})$ which denotes the acceleration due to a thruster system, the closed-loop system becomes

$$\dot{\boldsymbol{x}} = \boldsymbol{f}(\boldsymbol{x}, \boldsymbol{u}(\boldsymbol{x})) \qquad \boldsymbol{u} \in \mathbf{R}^m . \tag{2}$$

Based on a particular guidance law, a reference (target) state $\boldsymbol{x}^*$ is given and a scalar Lyapunov function $V(\boldsymbol{x}\text{-}\boldsymbol{x}^*)$ may be introduced to analyze the system's stability. Similar to the discussion of dynamic systems in terms of the scalar energy potential, Lyapunov's method proves the state $\boldsymbol{x}(t) = \boldsymbol{x}^*$ to be globally asymptotically stable, if a function $V(\boldsymbol{x}\text{-}\boldsymbol{x}^*)$ is found, which is continuous in its first derivative and satisfies the following conditions (Ilgen 1993)

$$V(\boldsymbol{0}) = 0 \tag{3}$$

$$V(\boldsymbol{x} - \boldsymbol{x}^*) > 0 \quad \forall (\boldsymbol{x} - \boldsymbol{x}^*) \neq \boldsymbol{0} \tag{4}$$

$$\dot{V}(\boldsymbol{x} - \boldsymbol{x}^*) < 0 \quad \forall (\boldsymbol{x} - \boldsymbol{x}^*) \neq \boldsymbol{0} \tag{5}$$

$$\lim_{\|\boldsymbol{x}-\boldsymbol{x}^*\| \to \infty} V = \infty . \tag{6}$$

Applied to the problem of relative motion control, Lyapunov's method may in principle be based on the Cartesian state vector, as well as on Keplerian or non-singular elements. It turns out, however, that the region in state space that could be controlled using a Cartesian formulation is much smaller than using Kepler elements (Naasz et al. 2002). Thus, in the following the state vector $\boldsymbol{x} = (a,e,i,\Omega,\omega,M_0)^T$ is considered.

Although Lyapunov's direct method does not comprise a procedure to construct the function $V(\boldsymbol{x}\text{-}\boldsymbol{x}^*)$, a quadratic positive-definite function is often an effective starting point, so

$$V(\boldsymbol{x} - \boldsymbol{x}^*) = \frac{1}{2}(\boldsymbol{x} - \boldsymbol{x}^*)^T \boldsymbol{K}(\boldsymbol{x}^*)(\boldsymbol{x} - \boldsymbol{x}^*) \tag{7}$$

where $\boldsymbol{K}$ is a positive definite gain matrix. It is obvious that (7) satisfies the Lyapunov conditions (3), (4) and (6). If we consider, furthermore, that the state vector time derivative is independent on the system dynamics in the absence of any control (as is the case for the Keplerian element state), we may write

$$\dot{\boldsymbol{x}} = \boldsymbol{g}(\boldsymbol{x})\boldsymbol{u} \tag{8}$$

where $\boldsymbol{g}$ is a matrix function of the state. Applied to orbital dynamics, Gauss's formulation of the Lagrange Planetary Equations (LPE) takes the form of (8) with

$$\frac{\partial}{\partial t}\begin{bmatrix} a \\ e \\ i \\ \Omega \\ \omega \\ M_0 \end{bmatrix} = \begin{bmatrix} \frac{2a^2 e s_\nu}{h} & \frac{2a^2 p}{hr} & 0 \\ \frac{p s_\nu}{h} & \frac{(p+r)c_\nu + er}{h} & 0 \\ 0 & 0 & \frac{r c_{\omega+\nu}}{h} \\ 0 & 0 & \frac{r s_{\omega+\nu}}{h s_i} \\ -\frac{p c_\nu}{he} & \frac{(p+r)s_\nu}{he} & -\frac{r s_{\omega+\nu} c_i}{h s_i} \\ \frac{p c_\nu - 2re}{na^2 e} & -\frac{(p+r)s_\nu}{na^2 e} & 0 \end{bmatrix} \begin{bmatrix} u_H \\ u_L \\ u_C \end{bmatrix} \tag{9}$$

where the acceleration vector components (u_H, u_L, u_C) are given in Hill's frame (Height, Along-track, Cross-track). Here $p = a(1-e^2)$, h denotes the orbital angular momentum and s_α and c_α denote the sine and cosine of the argument α. Based on (8) the derivative of Lyapunov's function can be written as

$$\dot{V}(\boldsymbol{x}-\boldsymbol{x}^*) = \frac{\partial V}{\partial \boldsymbol{x}}\dot{\boldsymbol{x}} = \frac{\partial V}{\partial \boldsymbol{x}}\boldsymbol{g}(\boldsymbol{x})\boldsymbol{u}. \tag{10}$$

If we furthermore set the control vector to be

$$\boldsymbol{u} = -\boldsymbol{g}^T(\boldsymbol{x})\left(\frac{\partial V}{\partial \boldsymbol{x}}\right)^T \tag{11}$$

the time derivative of Lyapunov's function becomes

$$\dot{V}(\boldsymbol{x}-\boldsymbol{x}^*) = -\left(\frac{\partial V}{\partial \boldsymbol{x}}\right)\boldsymbol{g}(\boldsymbol{x})\,\boldsymbol{g}^T(\boldsymbol{x})\left(\frac{\partial V}{\partial \boldsymbol{x}}\right)^T \tag{12}$$

which satisfies Lyapunov's condition (5). Based on a diagonal gain matrix, the Lyapunov function as given in (7) and applied to the control of the Keplerian elements is thus

$$V = \frac{1}{2}\left[K_1\delta a^2 + K_2\delta e^2 + K_3\delta i^2 + K_4\delta\Omega^2 + K_5\delta\omega^2 + K_6\delta M_0^2\right]. \tag{13}$$

This Lyapunov function satisfies the Lyapunov stability criteria for any system of the form as given in (8). Substituting the LPE into (11) leads to

$$\boldsymbol{u} = -\boldsymbol{g}^T(\boldsymbol{x})\left(\frac{\partial V}{\partial \boldsymbol{x}}\right)^T = -\begin{bmatrix} \frac{2a^2 e s_v}{h} & \frac{2a^2 p}{hr} & 0 \\ \frac{p s_v}{h} & \frac{(p+r)c_v + er}{h} & 0 \\ 0 & 0 & \frac{r c_{\omega+v}}{h} \\ 0 & 0 & \frac{r s_{\omega+v}}{h s_i} \\ -\frac{p c_v}{he} & \frac{(p+r)s_v}{he} & -\frac{r s_{\omega+v} c_i}{h s_i} \\ \frac{p c_v - 2re}{na^2 e} & -\frac{(p+r)s_v}{na^2 e} & 0 \end{bmatrix}^T \begin{bmatrix} K_1 \delta a \\ K_2 \delta e \\ K_3 \delta i \\ K_4 \delta \Omega \\ K_5 \delta \omega \\ K_6 \delta M_0 \end{bmatrix} \tag{14}$$

which exhibits the characteristics of Lyapunov's method to maintain a transparent relation between Keplerian element errors and the resulting control vector. However, it turns out that a proper selection of the six free control gain parameters K_i (i=1...6) is not a trivial task and still has to be solved in the sequel. Furthermore, to fully exploit the laws of orbital motion it turns out that mean anomaly errors are most efficiently removed by a change of the semi-major axis, which calls for a specific mean motion control. Both problems are addressed in the subsequent sections.

Gain Selection

While the derivation of the control law is relatively straightforward, the main difficulty in an appropriate implementation of the algorithm is the selection of the gain vector and the specification of the control on/off logic. This requires on one hand an educated guess of appropriate gain values and on the other hand extensive testing of the chosen values, similar to a Kalman filter tuning within orbit determination. One way is to relate the LPE in (9) with the achievable maximum changes in the orbital elements and the available control acceleration (Naasz 2002). This approach assures, that

1. Control is enforced only in such parts that effectively modify the orbital element
2. Control requests for different orbital elements are reasonably scaled w.r.t. each other
3. Control is enforced only when the orbital element error is above a certain threshold.

Although this approach is basically empirical, it provides a reasonable approach to arrive at suitable values for the gain vector. As a result, the following gain matrix has been derived to lowest order in eccentricity (Naasz 2002)

$$\boldsymbol{K}' = \frac{(n^* a^*)^2}{4\Delta t}\,\mathrm{diag}\left(\frac{1}{a^{*2}}, 1, 4, 4\sin^2 i^*, e^{*2}, e^{*2}\right) \tag{15}$$

where Δt is the thrust duration and the star refers to the reference orbit. Basically, the gains in (15) are not varying with time. However, use of time varying gains can be made to encourage certain orbit element corrections to occur during particular phases of the orbit. From the LPE it is concluded, that the response to thrusts for the argument of perigee is shifted by 90° as compared to changes in the semi-major axis and

eccentricity, which are encouraged at apogee and perigee. Thus the gains for the in-plane elements may be varied depending on the true anomaly v* of the reference orbit according to

$$\begin{aligned} K_1 &= K_1' \left|\cos(v^*)\right| \\ K_2 &= K_2' \left|\cos(v^*)\right| \\ K_5 &= K_5' \left|\sin(v^*)\right|. \end{aligned} \tag{16}$$

To prevent thrusting when the orbital element deviations are too small to require activation of the thruster, a velocity increment of

$$\Delta \boldsymbol{v} = \frac{T}{m}\frac{\boldsymbol{u}}{|\boldsymbol{u}|}\Delta t \tag{17}$$

is applied only when $|\boldsymbol{u}|$ exceeds the threshold T/m, where T is the available thrust level from the actuator and m is the spacecraft mass. No specific spacecraft thrust model is assumed, where a thruster on/off logic would apply for each thrust direction individually.

Mean Motion Control

Lyapunov's method, as given in (14), provides a working control law for satellite formations. However, a modification for enhanced efficiency may be obtained, when we consider that mean anomaly errors δM could be corrected for by a change of the semi-major axis, affecting the mean motion. This approach, also termed as mean motion control, fully exploits the laws of orbital motion to reduce in-plane errors. Furthermore, it reduces the control problem from a six-dimensional control state by one dimension at the expense of complicating the semi-major axis control. The dynamics of relative mean anomaly are, using $dM/dt = n$, given as

$$\frac{d}{dt}(\delta M) = n - n^* = \sqrt{\frac{GM}{a^3}} - \sqrt{\frac{GM}{a^{*3}}} \tag{18}$$

where GM denotes the Earth's gravitational coefficient. A suitable approach to minimize the mean anomaly error is given by

$$\frac{d}{dt}(\delta M) = -K\delta M \tag{19}$$

with some positive gain K. Using (18) and (19) we can solve for the semi-major axis a, which removes the mean anomaly error by a suitable chosen modified target semi-major axis a^{**} according to

$$a^{**} = \left(a^{*-3/2} - \frac{K\delta M}{\sqrt{GM}}\right)^{-2/3} \tag{20}$$

which reduces to a^* for vanishing δM. Since the required modification of the semi-major axis due to mean anomaly errors is small as compared to the semi-major axis itself, a first-order Taylor series expansion leads to

$$a^{**} \approx a^* + \frac{2}{3}\frac{K\delta M a^*}{n^*}. \tag{21}$$

Hence, if we replace $\delta a = a - a^*$ by $\delta a^* = a - a^{**}$ in (14), we obtain the along-track control law due to semi-major axis and mean anomaly errors as

$$u_L \approx \frac{K\delta M a^*}{3\Delta t} - \frac{\delta a n^*}{2\Delta t}. \tag{22}$$

Thus, the along-track control acceleration may conveniently be written as the sum of a component due to mean anomaly errors (first term) and due to semi-major axis errors (second term). Considering a scenario just with an initial along-track position difference of δL_0, the total initial along-track control is due to the mean anomaly error. As consequence, a semi-major axis offset δa is built up until the two contributions balance. In the sequel, the semi-major axis error has to be removed again to stop the drift and arrive at the targeted along-track position.

An appropriate selection of the mean motion gain K is particularly simple, if we consider impulsive velocity increments from a thruster system, not constrained in magnitude. To this end, an along-track offset δL is considered which may be removed by a semi-major axis offset of δa accumulated over a time t_c, according to

$$\delta L = \delta M a^* = 3\pi\delta a \frac{t_c}{T^*} \tag{23}$$

with the orbital period T^*. When (23) is inserted into (22) an expression for K is obtained

$$K = \frac{n^*}{2\pi}\frac{T^*}{t_c} = \frac{1}{t_c}. \tag{24}$$

Thus, the mean motion gain for unconstrained thrusters is simply given by the inverse of the characteristic time t_c, over which the mean motion control should accumulate along-track offsets. The shorter the time for along-track offset compensation should be, the higher we have to choose the mean motion gain and the more aggressive is the mean motion control. For a Low-Earth Orbit satellite, a mean motion gain of $K = 1.4 \cdot 10^{-4}$/s would remove along-track errors in a period of about 120 min.

AUTONOMOUS FORMATION FLYING DEMONSTRATION

Simulation Setup

The formation consists of two spacecraft, flying in a polar Low Earth Orbit of 87° inclination and 450 km altitude, which involves a strongly varying GPS satellite visibility and notable signal dynamics. A close formation with an initial along-track separation of 800 m is considered.

A pulsed plasma thruster (PPT) system has been selected which can be accommodated on a small satellite (Cassady et al. 2000). In a doubled configuration the thrusters provide an impulse-bit of 0.112 mNs and fire at a rate of 1 Hz. In the framework of the simulations, an effective thrust level of 0.1 mN and a spacecraft mass of 20 kg is assumed. Thrust accelerations are accumulated over 10 s intervals to arrive at velocity increments to be applied instantaneously to the current satellite velocity. Although specific satellite designs may significantly constrain available thrust directions, no such constraints were considered in the present setup.

As part of the simulation system the satellite orbits are propagated by a precision software propagator running on the Remote Control PC. It applies the numerical integration algorithm DE of variable order and stepsize (Shampine & Gordon 1975) to integrate the equations of motion in an Earth-Centered Earth-fixed (ECEF) frame. As the DE method provides interpolation for dense output it is ideally suited to support the required 100 ms period of motion messages to the GPS signal simulator. Furthermore, use of the ECEF system for integration avoids frequent coordinate transformations between an inertial system and the ECEF system, which is the system to be applied for motion messages.

The adopted force model accounts for the Earth's complex gravity field by using a 20x20 subset of the Joint Gravity Model 3 (JGM-3). Furthermore, it accounts for perturbations due to atmospheric drag, solar radiation pressure, as well as sun and moon third body perturbations. In addition to the natural perturbations, orbit maneuvers are accounted for by adding velocity increments in the ECEF frame to the ECEF velocity components of the respective state vector. A summary of the simulation setup is given in Table 1.

Table 1. CONFIGURATION OF THE FORMATION FLYING SYSTEM.

Subsystem	Description
Remote Control PC	
Earth gravity field	20x20 subset of JGM-3 model
Atmospheric drag	modified Harris Priester model
Solar radiation pressure	Spherical model
Sun third body force	Analytic sun ephemeris
Moon third body force	Analytic moon ephemeris
Numerical integration algorithm	DE variable order and stepsize
Reference system for integration	WGS-84
GPS Signal Simulator	
Ionospheric errors	Based on constant TEC of 20 TECU
GPS broadcast ephemeris errors	Maximum of 12 m per component
Navigation Processor	
Applied GPS measurements	Absolute & relative navigation solutions
Number of thrusting spacecraft	2
Control cycle period	10 s

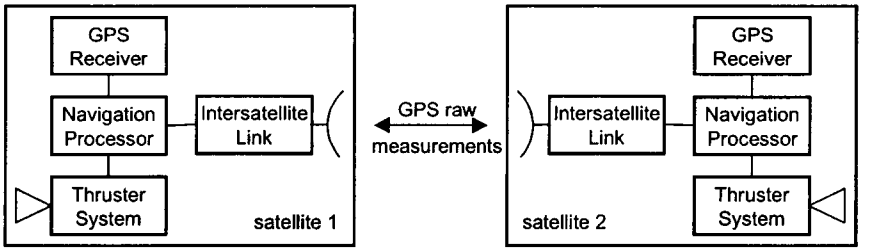

Fig. 2. Space segment of a formation with two thrusting spacecraft.

To demonstrate the autonomous control concept in the presence of realistic GPS signals, systematic ionospheric errors and GPS broadcast ephemeris errors were modeled in the GPS signal simulator and applied for the generation of GPS signals. Ionospheric errors were based on a total electron content of $2 \cdot 10^{17}$ electrons/m^2 (= 20 TECU). Intentional GPS broadcast ephemeris errors have been added with maximum values of 12 m per component, as derived from observed offsets between GPS broadcast ephemerides and precise IGS ephemerides for the simulation date.

A symmetric space segment is assumed with two thrusting spacecraft as indicated in Fig. 2. The intersatellite link has been replaced in the hardware setup by the direct connection of the two GPS receivers through a dedicated serial link. While a generic concept would perform the relative navigation solution within the navigation processors, the Orion feature to provide the relative navigation solutions has been utilized instead. In order to emulate two independent navigation processors on a single flight computer, two separate control threads have been implemented on the Power PC. It is noted, that no control vectors have to be exchanged between the two spacecraft according to the guidance concept described in the following section.

Guidance Concept

The adopted formation control algorithm requires the absolute current and target state of the formation as input. While the absolute current state vector of the spacecraft is readily available from its GPS position and velocity fixes, the derivation of an appropriate target state is part of the guidance problem of formation flying. Although this problem might be solved by numerically integrating a reference trajectory, this approach is inefficient since it requires a high computational effort on the navigation processor. Furthermore it is not flexible, since the guidance is defined with respect to a fixed trajectory.

In general, guidance of a formation may well be separated into guidance with respect to the absolute orbit of one of the spacecraft and guidance with respect to the relative formation geometry. Scientific or technological objectives of a formation flying mission are in fact in many cases only related to the relative formation geometry.

Thus, for a formation separated in along-track direction with spacecraft 1 preceding spacecraft 2 and a positive target separation of ΔL, the target elements for the first spacecraft are the current elements of the second spacecraft, except for the mean anomaly, which is

$$M_1^{\text{target}} = M_2 + \frac{\Delta L}{a_2} \tag{25}$$

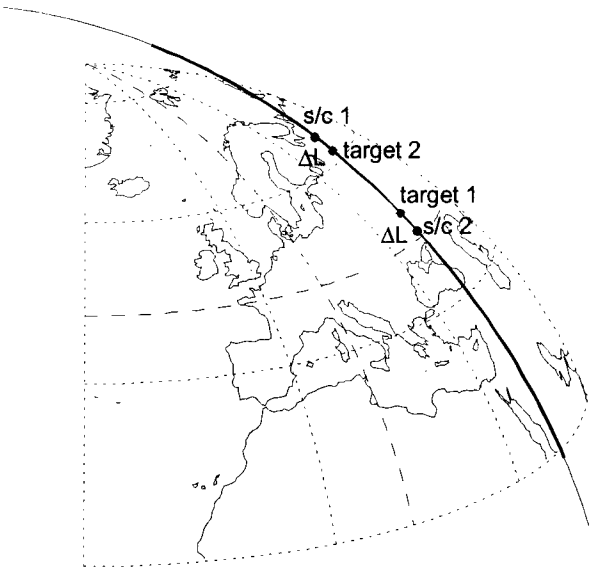

Fig. 3. Guidance strategy for formations separated in along-track direction by ΔL. The target states for spacecraft 1 and 2 (black) are denoted by 1_t and 2_t (gray).

where the indices refer to the two spacecraft. It is important to note that a control of the osculating motion of the formation in the presence of a realistic force model is effectively avoided by replacing the osculating current and target states in the control by a suitable set of mean elements, e.g. using the algorithm of Brouwer (1957) modified by Lyddane (1963). This guidance approach based on the relative formation geometry has the following characteristics:

1. Guidance depends on absolute current states and relative target formation geometry
2. Dynamic guidance law separates the absolute and relative guidance problem
3. Numerical integration of the target trajectory is avoided
4. Measurement-driven absolute state errors do not affect the control to first order.

In the conducted demonstration, this approach has been extended to allow both spacecraft to be active and control the formation in parallel as indicated in Fig. 3. Although not fuel optimal, this concept allows for a completely autonomous and dynamic acquisition of the final formation geometry. Even if one spacecraft's thruster system would fail, no ground intervention would be required to achieve the target relative formation geometry in this case.

Results from the Hardware-in-the-Loop Demonstration

A hardware-in-the-loop (HWIL) demonstration of closed-loop autonomous formation control has been performed based on the above described setup. In the course of the demonstration which covers a period of 12 hours, the initial along-track separation of 800 m is effectively removed by changing the relative mean semi-major axis of the two orbits, as indicated by the height component in Fig. 4.

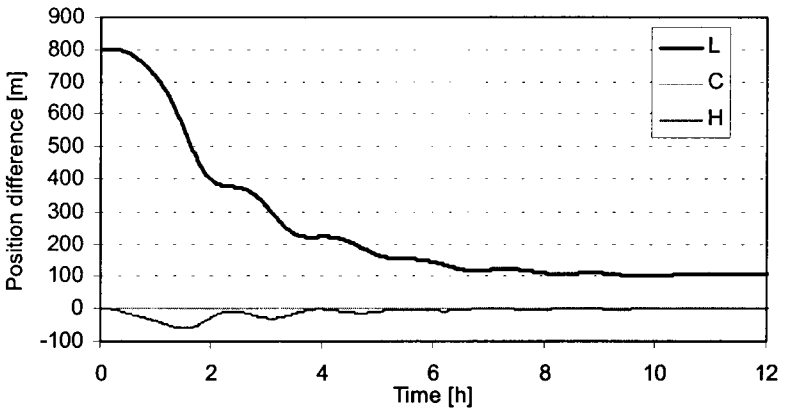

Fig. 4. Demonstration of closed-loop autonomous formation control. The initial along-track separation is decreased to the target separation of 100 m.

Following a coarse acquisition of the target formation within 8 hours into the demonstration, the formation keeping starts at about 9.5 hours after start of the simulation. The performance of the control algorithm for formation keeping may be evaluated by the maximum, mean and standard deviation figures of the current spacecraft state with respect to the target state. A summary of the formation keeping results in the orbital frame components (*L*, *C*, *H*) and relative position (*R*) covering a period of 2.5 hours is given in Table 2.

Table 2. CHARACTERISTICS OF AUTONOMOUS FORMATION KEEPING CONTROL.

	L [m]	*C* [m]	*H* [m]	*R* [m]
Minimum	100.3	-0.1	-2.7	100.3
Maximum	111.1	0.1	1.5	111.1
Mean	106.2	0.0	-0.3	106.2
RMS	2.8	0.1	1.1	2.8

Thus, the targeted along-track separation of 100 m was kept with a mean position error of about 6 m and a standard deviation of 3 m.

Performance Analysis

The above results demonstrate that the closed-loop system and the applied control algorithm are working well for autonomous formation control. In the following section, the performance of the system is addressed in terms of the achieved GPS measurement accuracy, the computational load on the navigation processor, and the fuel consumption.

GPS Performance

The Orion absolute navigation solutions derived from pseudorange measurements exhibit a typical data noise of 1 m and 0.5 m/s in the absence of systematic errors. With broadcast ephemeris errors, the resulting position errors are directly proportional to the assumed ephemeris errors and amount to 5–10 m for an S/A free scenario. The high level of common error cancellation reduces the errors of the relative navigation solutions to σ_p^r = 0.6 m and σ_v^r = 0.005 m/s even in the presence of systematic errors.

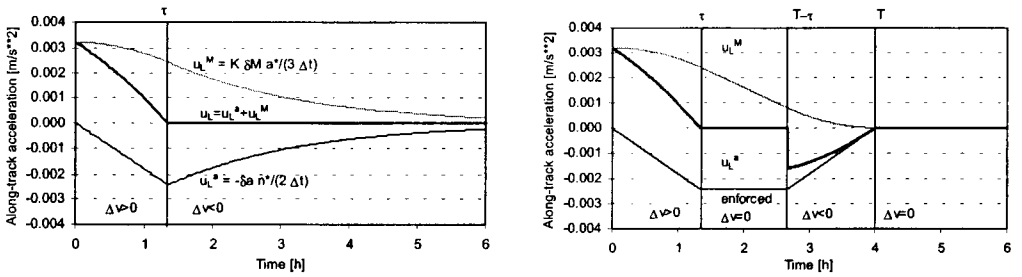

Fig. 5. Along-track control requests in the formation acquisition phase. Gain scheduling is absent in the left figure and present in the right figure.

Computational Load on the Flight Computer

The computational load on the navigation processor is governed by the computation of the mean elements and the control vectors. The computation of mean elements based on the Brouwer/Lyddane algorithm requires about 50 ms per element set, comparable to the computation of mean elements using the SGP4 algorithm. Thus, the computational load for mean element computation of two satellites is 100 ms. The control algorithm including the computation of the control gains takes 50 ms, hence a total of 150 ms is required per execution of the control thread, which is evoked every 10 s. As the absolute and relative GPS navigation solutions are applied, no dynamical smoothing or numerical trajectory integration is required. Thus the implemented concept proves to be very efficient, requiring only about 1.5% of the navigation processor resources.

Fuel Consumption during Formation Acquisition

An almost continuous thruster firing is observed in the formation acquisition phase. This is caused by a lacking drift phase, present in the classical burn-coast-burn scenario, and a thruster on/off logic which is very susceptible to GPS measurement noise. This is illustrated in the left diagram of Fig. 5. Here, the along-track acceleration and its components due to mean anomaly and semi-major axis errors are displayed according to (22). Continuous thrust in the first phase is requested almost entirely due to the mean anomaly error. As a consequence, an intentional semi-major axis error is built up until the two contributions almost cancel each other. Subsequently, a delicate balancing of the two decreasing components is observed which nevertheless results in a residual net acceleration, sufficient to pass the thruster on/off logic. Thus, the drift is reduced almost immediately after it has been built up and reduces gradually until the formation keeping phase is entered.

Instead of a permanent thrusting, a dedicated drift phase can be enforced by an appropriate gain scheduling. To this end, the gain is set to zero in the drift interval $[\tau, T - \tau]$ where T is the acquisition period and τ is thruster activity period according to

$$\tau = \frac{T}{2} - \sqrt{\frac{T^2}{4} - \frac{\Delta L_0}{3u_{s/c}}} \tag{26}$$

where $u_{s/c}$ is the thrust acceleration and ΔL_0 is the initial along-track offset from the target. As a consequence, the semi-major axis stays constant during the coast phase as seen in the right diagram of Fig. 5. At the end of the coast phase, the semi-major axis

offset causes a strong request for drift stop, which dominates the measurement noise and, thus, renders the formation acquisition phase essentially independent from measurement noise. Instead of choosing an arbitrary acquisition period T, the elapsed time between the center of the two burns, $T - \tau$, may be chosen as an integer number of orbits, thus avoiding relative eccentricity errors at the end of the acquisition phase. In the above example with T = 4 h, the required velocity increment for the acquisition phase with gain scheduling is 0.048 m/s, matching that of the conventional burn-coast-burn strategy, as opposed to 0.144 m/s without gain scheduling.

Fuel Consumption during Formation Keeping

The GPS measurement noise of the relative navigation solution dominates in particular the formation keeping phase. This is obvious when we compare the acceleration threshold T/m, being $5 \cdot 10^{-6}$ m/s^2 for the considered case, with the quotient of the relative velocity noise and the thrust accumulation interval $\sigma_v^r/\Delta t$, which is $5 \cdot 10^{-4}$ m/s^2. As a consequence, a permanent thrusting is observed which renders the control ineffective. Two approaches may basically solve the problem: a decrease of the data noise and an increase of the thrust accumulation interval. Since the data noise may, additionally, be reduced by an averaging algorithm over the interval Δt, the noise scales with $\Delta t^{-1/2}$. In order to improve the control noise of acceleration by a factor of 100, Δt should be changed by a factor of $100^{2/3} \approx 22$ from 10 s to about 3.5 min. Verification of noise reduction techniques are therefore among the next steps to be performed.

CONCLUSIONS

A hardware-in-the-loop demonstration of real-time autonomously controlled closed-loop formation flying has been performed. To that end, two interconnected GPS receivers delivered their absolute and relative navigation solutions to a flight computer, which derived the necessary control vectors for the autonomous formation acquisition and keeping. The guidance law has been formulated completely in relative navigation terms, thus avoiding any numerical integration of the reference trajectory on the flight computer and rigorously separating absolute and relative control of the formation. The control vectors were computed based on Lyapunov's direct method modified for mean motion control to fully exploit the laws of orbital mechanics for along-track separated satellite formations.

A sample scenario was considered consisting of two micro-satellites in a near-polar Low Earth Orbit, separated initially in along-track direction by 800 m. Making use of a pulsed plasma thruster system on each satellite, the autonomous acquisition and subsequent keeping of the formation with two active spacecraft controlling dynamically their relative geometry has been demonstrated. The formation acquisition phase ended at about 8 h into the simulation, when the satellites achieved their targeted along-track separation of 100 m. Making use of a realistic force model and accounting for typical systematic ionospheric and broadcast ephemeris errors, a formation keeping accuracy of about 3 m (3D rms) has been obtained. According to a generic requirement, the control accuracy of a formation should be at least one tenth of the minimum spacecraft separation. Thus, the demonstration proved the feasibility of the autonomous control of a satellite formation down to a minimum separation of at least 50 m. The achieved results are considered of relevance in the field of autonomous navigation and enhance potential mission scenarios for upcoming formation flying missions.

ACKNOWLEDGEMENT

The described system has been established at the Formation Flying Test Bed at NASA's Goddard Space Flight Center (GSFC). Work was carried out from June to September 2002 in the framework of a DLR sabbatical. T. Stengle's support and organization of the sabbatical at GSFC is greatly acknowledged. R. Burns is thanked for helpful discussions on the subject and L. Jackson for his support to establish the system interfaces.

REFERENCES

Bleeker J., Mendez M.; *The XEUS Mission*; Proc. Symposium *New Visions of the X-ray Universe in the XMM-Newton and Chandra Era* 2, ESTEC, The Netherlands, ESA SP-488 (2002).

Brouwer D.; *Solution of the Problem of Artificial Satellite Theory Without Drag*; The Astronautical Journal **64**, 378-397 (1957).

Cassady R.J., Hoskins A.W., Campbell M., Rayburn C.; *A Micro-Pulsed Plasma Thruster for the Dawgstar Spacecraft*; Proceedings of the 2000 IEEE Aerospace Conference, Big Sky, Montana (2000).

Chapman P., Gillett L.; *Formation Control for Darwin Demonstration in the SMART-2 mission;* International Symposium Formation Flying Mission and Technologies, Toulouse, France (2002).

Chien S., Sherwood R., Burl M., Knight R., Rabideau G., Engelhardt B., Davies A., Zetocha P., Wainwright R., Klupar P., Cappelaere P., Surka D., Williams B., Greeley R., Baker V.; *The Techsat-21 Autonomous Sciencecraft Constellation*; ESA Workshop on On-board Autonomy, WPP-191, Noordwijk, The Netherlands (2001).

Ilgen M.R.; *Low Thrust OTV Guidance Using Lyapunov Optimal Feedback Control Techniques*; AAS/AIAA Astrodynamics Specialist Conference Victoria, Canada (1993).

Leitner J.; *A Hardware-in-the-loop Testbed for Spacecraft Formation Flying Applications*; 2.0908, IEEE Aerospace Conference, Big Sky, MT (2001).

Leung S., Gill E., Montenbruck O., Montenegro S.; *A Navigation Processor for Flexible Real-Time Formation Flying Applications*; International Symposium Formation Flying Mission & Technologies, 29-31 October 2002, Toulouse, France (2002).

Lyddane R.H.; *Small Eccentricities or Inclinations in the Brouwer Theory of the Artificial Satellite*; The Astronomical Journal **68**, 555-558 (1963).

Montenbruck O., Markgraf M., Leung S., Gill E.; *A GPS Receiver for Space Applications*; B1-Ax; ION GPS 2001 Conference, Salt Lake City, 12-14 Sept. 2001 (2001).

Montenbruck O., Ebinuma T., Lightsey E.G., Leung S.; *A Real-Time Kinematic GPS Sensor for Spacecraft Relative Navigation*; Aerospace Science and Technology **6**, 435-449 (2002).

Montenegro S.; *Spacecraft Bus Computer*; BIRD Spacecraft Description **3**, TN-BIRD-5800-GMD/073 DLR (2001).

Naasz B.J., *Classical Element Feedback Control for Spacecraft Orbital Maneuvers*, Virginia Polytechnic Institute and State University, Master Thesis (2002).

Naasz B.J., Karlgaard C.D., Hall C.D.; *Application of Several Control Techniques for the Ionospheric Observation Nanosatellite Formation*, AAS 02-188; AAS/AIAA Space Flight Mechanics Meeting, San Antonio, Texas, Jan. 27-30 (2002).

Ries J.C., Tapley B.D., Bettadpur S.; *The GRACE Mission: Status and Plans*; DDA 33rd Meeting, Mt. Hood, OR, (2002).

Rossi M., Lovera M.; *A Predictive Approach to Formation Keeping for Constallations of Small Spacecraft in Elliptical Orbits*; 5th International ESA Conference on Guidance Navigation and Control Systems, October 22-25, Frascati Italy (2002).

Shampine L.F., Gordon M. K.; *Computer Solution of Ordinary Differential Equations*; Freeman and Comp., San Francisco (1975).